Techset Composition Ltd, Salisbury
Doc: {IEE}OPT/Articles/Pagination/OPT20110044.3d

www.ietdl.org

Published in IET Optoelectronics
Received on 2nd June 2011
Revised on 3rd August 2011
doi: 10.1049/iet-opt.2011.0044

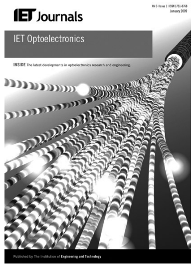

ISSN 1751-8768

Simultaneous measurement of thickness and refractive index by a single-channel self-mixing interferometer

M.T. Fathi S. Donati

Dipartimento Elettronica, Universita' di Pavia, 27100 Pavia, Italy
E-mail: silvano.donati@unipv.it

Abstract: The authors introduce a new method for the simultaneous measurement of thickness d and refractive index n of transparent slabs and thin films. The method is based on the optical phase shift measured by a single-channel, self-mixing interferometer (SMI) as a function of the angle of incidence on the sample. The authors use a motorised rotating stage to apply an angular scan up to $\pm 65^\circ$ to the sample. Then, the authors analyse the derivative of phase difference with respect to the rotation angle, apply a standardisation and fit it to the theoretical expression and after a few iterations they are able to simultaneously determine n and d, with a typical accuracy of 0.02 and 1%, respectively.

1 Introduction

Recently, we reported on a method to measure the thickness and index of refraction of a transparent slab, based on the use of a two-channel interferometer set-up. In the set-up, one channel was a forward-path lateral shear interferometer (LSI) [1], looking at the superposition of the two beams marked full line and dotted line in Fig. 1 and the other channel was a self-mixing interferometer (SMI), looking at the beam reflected back to the laser source, go-and-return full-line in Fig. 1. As shown in [2], the difference of the two phase-shift readouts (LSI and SMI) is a phase term only dependent on d, and thus firstly, the method allows us to determine thickness d independent from refractive index n. Secondly, we reuse the LSI (or SMI) phase shift, insert d in the equation and are able to solve for n as well. The method actually works well, especially for determining thickness d, yet has a limitation: the superposition of lateral waves in the LSI channel decreases in amplitude at large angles and this limits the maximum angular swing and hence the resolution we can obtain, affecting the index of refraction determination. Instead, the SMI signal is good also at large rotation angles, up to $\simeq 65^\circ$, because it is
Q1 obtained by a forward-moving beam and has no lateral beam shift. Removing the second channel is not trivial, however, because it is crucial [2] to eliminate the index of refraction from the calculation of thickness.

Thus, to improve the measurement method further, and be able to simultaneously measure thickness and refractive index using a single-channel SMI, we had to rethink the algorithm to treat measured data, starting back from the interferometric signal. In particular, we find that processing the derivative of the SMI phase difference at large angles (30–60°) yields a clean waveform with increased information content, leading to an effective calculation routine to extract thickness and refractive index from the measured data. The results obtained with the new approach show a better resolution compared to our previous work [2], as will be presented below.

About the SMI, several papers describing this new method of optical phase shift measurement have been published [3–6]. Just to recall its key features, we can say that SMI is based on the coherent interaction of the cavity field and the (weak) optical field re-entering the laser cavity after propagation to a remote reflector (or diffuser) and back. The interaction generates modulations of both amplitude (AM) and frequency (FM) of the in-cavity optical field. While the FM is difficult to detect because impressed on the very high optical frequency, the AM term is readily available by looking at the optical power $P \cong E^2$ emitted by the laser. In the SMI, under the re-injection regime, the emitted power is $P(\varphi) = P_0[1 + mF(\varphi)]$, where P_0 is the power of the unperturbed LD, m is the AM modulation index (or relative strength) of the self-mixing process and $F(\varphi)$ is a periodic function of the optical phase shift $\varphi = 2ks$ of the external path to the remote target and back, where s is the target distance, $k = 2\pi n/\lambda_0$ is the wavenumber of propagation in the external medium of index of refraction n and λ_0 is the wavelength of the laser (in vacuum). The actual shape of function $F(\varphi)$ depends on the feedback parameter C [3, 4] which in turn depends on laser parameters, target distance and mirror reflectivity, but interestingly for small C ($\ll 1$) $F(\varphi)$ is a cosine function, whereas the FM is a sine function of the external phase shift φ [3, 4].

For measurement purposes, we always keep the SMI signal in the weak regime ($C \ll 1$) by appropriate attenuation, so that $F(\varphi) = \cos \varphi$, like expected in a normal interferometer. The AM is converted into an electrical signal by a photodiode, and conveniently we use the one already provided by the manufacturer for power monitoring,

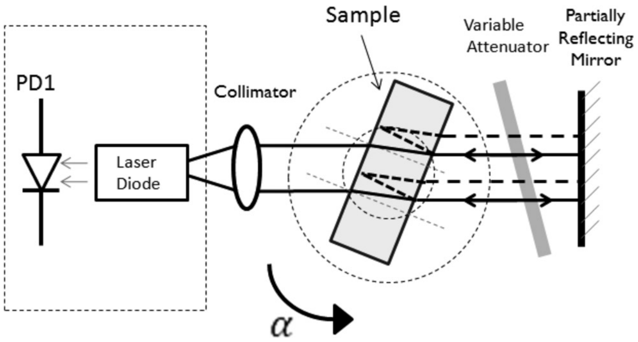

Fig. 1 *Experimental set-up: a collimated laser beam is sent through the sample under test, up to a remote target made up by a partially reflecting mirror*

Reflected beam retraces the forward path back to the laser cavity, and is received by photo-detector placed behind of laser diode, where it generates the SMI interferometric signal cos $\Delta\varphi$

mounted in the device package at the rear mirror location. The photodiode collects the emission from the back mirror and yields a photocurrent proportional to cos $2ks$, which is readily amplified and made available for further processing.

Features of the SMI are: (i) inherent self-alignment, (ii) no need for stray-light filters nor for spatial filters to correct wave-front distortion and (iii) high sensitivity typical of a coherent detection. The requirements for good operation of the SMI are: (i) a single-mode diode laser, with good (>30 dB) side mode suppression shall be used, (ii) distance s shall be less than the coherence length of the unperturbed laser and (iii) return shall be small (in the 10^{-6}–10^{-3} range of relative power, that is, of signal power to emitted beam power) for operation to be in the linear regime [7]. Too large a strength of returning power can in fact drive the laser out of the SMI weak coupling, into the chaos-generating regime, useful for optical cryptography but not suitable for linear, measurement-related applications. All the above conditions are easily met, in practice, and in the following we present an application fully satisfying all of them, namely with the laser working in the SMI weak-coupling regime.

2 Self-mixing interferometer channel

In the SMI set-up (Fig. 1) collimated beam from a laser diode (LD) is passed through the sample under measurement, and a small fraction (about 0.5×10^{-3} in power) of the optical field, is reflected back and allowed to re-enter the laser cavity. In practice, to obtain $C \ll 1$, we need to attenuate the ongoing or back-reflected beam by a factor of about 10^{-2} (in power) in addition to the normal (moderate) attenuation we find in the set-up, because of propagation and diffraction losses, partial reflectivity of the target and mode superposition loss at the cavity. About the optical path, rays reflected back by the remote mirror re-trace the optical path exactly, making identical the go-and-return paths (with some beam broadening for diffraction) up to the point of rays re-entering the LD cavity. Specifically, the phase shift φ read by the SMI is made up by three terms, for the paths: laser to sample front surface, front-to-back sample surfaces, sample back surface to target (and reverse paths). At normal incidence ($\alpha = 0$) the total phase shift is $\varphi(0) = 2ks + (n-1)d$, d and n being sample thickness and index of refraction, and s is the target mirror distance from the laser (in a path with $n = 1$). Upon rotation of the sample from 0 to a certain α, the optical phase shift $\varphi(\alpha)$ changes, mainly because of the increased path suffered upon crossing the sample. The dependence of the phase difference $\Delta\varphi = \varphi(\alpha) - \varphi(0)$ from the rotation angle α is worked out with some algebra as [2]

$$\Delta\varphi = 2kd(n\cos\theta - \cos\alpha) \tag{1}$$

where θ is the internal refraction angle (Fig. 1). The main dependence of $\Delta\varphi$ is from optical thickness kd, as it is usually found in interferometric-based measurements. Only a minor dependence is on n because of the second term in parentheses, on the right-hand side of (1), and this is the deviation we are going to exploit to be able determining both n and d from experimental data of an SMI. In contrast, if a second channel of phase is available (the LSI as in [2]), the task is much easier because subtracting the two phases yields an equation of the type $\Delta\varphi = 2kd\cos\alpha$ (being k the in-vacuum value), independent from n.

3 Experimental set-up

In the experiment, we use a laser diode as the source, a GaAlAs triple-QW semiconductor laser from Hitachi (HL8325G), emitting up to 20 mW at $\lambda = 832$ nm on a single longitudinal mode with a good side mode suppression (typ. 35 dB). The diode laser was fed by a constant current supply, and temperature controlled by a TEC module to avoid mode hopping. The photodiode was terminated on high-Z trans-impedance op-amp (with feedback resistance $R_F = 300\ \mathrm{k\Omega}$) to ensure reasonable bandwidth (100 kHz) and low noise of the detected SMI signal. A collimating objective (polymer) lens supplied by the manufacturer gives a nearly circular spot with 1-mm diameter. The partially reflecting mirror used a semi-transparent thin cover-glass metalised with a reflectance $R = 70\%$, and was mounted on a micro-positioning stage placed at a $s = 40$ cm distance from the laser source, whereas the sample under test was placed at about 20 cm. The sample was mounted upon a rotating dc motor running at constant speed (typ. 700°/s), adjustable by a voltage control. Residual misalignment in the rotating set-up limits the maximum useable angular swing to about $\pm 65°$.

A variable attenuator have been used to keep the feedback at a relative power level of ~ 0.2–0.5×10^{-3} typically, so that $C \ll 1$, and the photodiode signal is $I = I_0(1 + \cos\Delta\varphi)$, with $\Delta\varphi$ given by (1). In Fig. 2, we report the experimental cos $\Delta\varphi$ signal of the SMI (top diagram), and the plot of the phase $\Delta\varphi$ extracted from the peaks (maxima and minima) of it (bottom), showing a clean trend, nearly parabolic, as a function of rotation angle α. Note also that, while cos $\Delta\varphi$ has some amplitude noise and uneven peak-to-peak amplitude, the $\Delta\varphi$ diagram is much cleaner (because related to phase, not to power).

Also to remark, we found that the results are relatively unaffected by changes of distances of target mirror and of sample from the laser (they may go up to 2 m and more if simple readjustment of attenuation is used to keep the feedback level constant).

4 Derivative of phase difference

To extract d and n from the experimental data of Fig. 2*a*, one can think of matching the experimental interferogram (Fig. 2*a*) to the analytical expression (1), by an LMS

doi: 10.1049/iet-opt.2011.0044

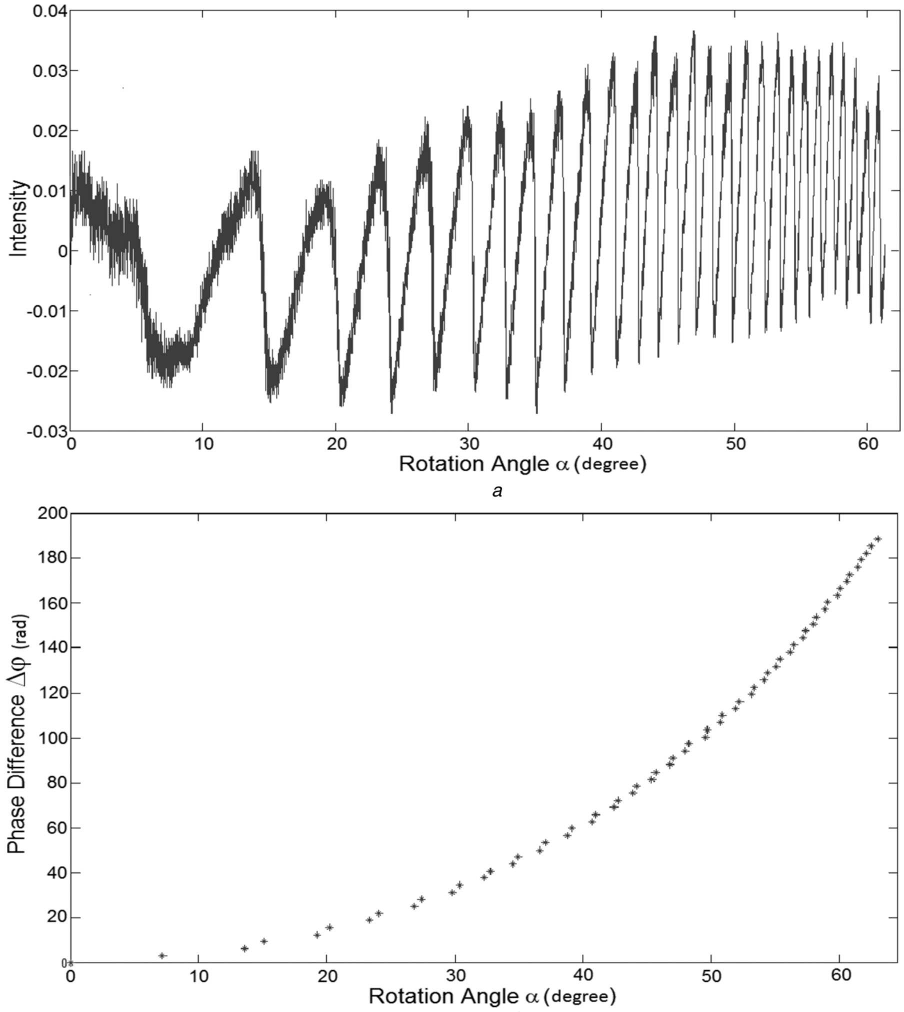

b

Fig. 2 *Typical experimental signal and phase as a function of the rotation angle* α

a Signal $\cos \Delta\varphi$
b Phase $\Delta\varphi$
Fringe frequency increases with α, while amplitude is not constant because of small misalignments. Data are for $n = 1.34$ and $d = 55$ μm Q2

minimisation or other well-known cost-based algorithms [5]. Doing so, however, we found results much dependent on pre-filtering of data. Indeed, looking at the waveform of Fig. 2*a*, we see that the peak-to-peak amplitude and also the average baseline change appreciably with angle α (both should be constant, theoretically). This causes the error by large. On the other hand, as the peak extraction removes both dependences, it looked like an almost-optimal pre-filtering and we continued on the idea of handling the data in an analogue format. As the trend of phase (Fig. 2*b*) is nearly parabolic, we followed the idea of extracting the slope from it. Now, the derivative of SMI phase difference with respect to α is calculated from (1) and using $n \sin\theta = \sin\alpha$, as

$$\phi'(\alpha) = \frac{\mathrm{d}(\Delta\varphi)}{\mathrm{d}\alpha} = \frac{-kd}{n}\sin^2\alpha\left(1 - \frac{1}{n^2}\sin^2\alpha\right)^{-(1/2)} + 2kd\sin\alpha \quad (2)$$

Fig. 3*a* shows $\phi'(\alpha)$ with respect to the rotation angle α for a wide range of refractive index. As the trend of $\Delta\varphi$ with α is smooth, the derivative $\phi'(\alpha)$ can be calculated numerically as the incremental ratio

$$\phi'\left(\frac{\alpha_2 + \alpha_1}{2}\right) = \frac{\Delta\varphi(\alpha_2) - \Delta\varphi(\alpha_1)}{\alpha_2 - \alpha_1} \quad (3)$$

where $\alpha_1 = \alpha - \Delta\alpha/2$ and $\alpha_2 = \alpha + \Delta\alpha/2$ are limits of incremental ratio around α and $\Delta\alpha$ is the incremental step, taken equal to the quantisation interval of the experimental data (Fig. 2*b*). Then, $\phi'(\alpha)$ can be fitted by a polynomial curve using least-squares approximation. As more fringes are found at large angles, the derivative allows a good curve fitting and easy smoothing of experimental data. The result of calculation for $n = 1.34$, $d = 55$ μm is shown in Fig. 3*b*.

Now, let us standardise $\phi'(\alpha)$ by dividing it by factor kd, and then subtract $2\sin\alpha$. Doing so, we obtain

$$\phi'_s(\alpha) = \frac{1}{\mathrm{kd}}\phi'(\alpha) - 2\sin\alpha = -\frac{1}{n}\sin^2\alpha\left(1 - \frac{1}{n^2}\sin^2\alpha\right)^{-(1/2)} \quad (4)$$

Function $\phi'_s(\alpha)$ is now made independent from kd and is only weakly dependent on n. We can now attempt to match the

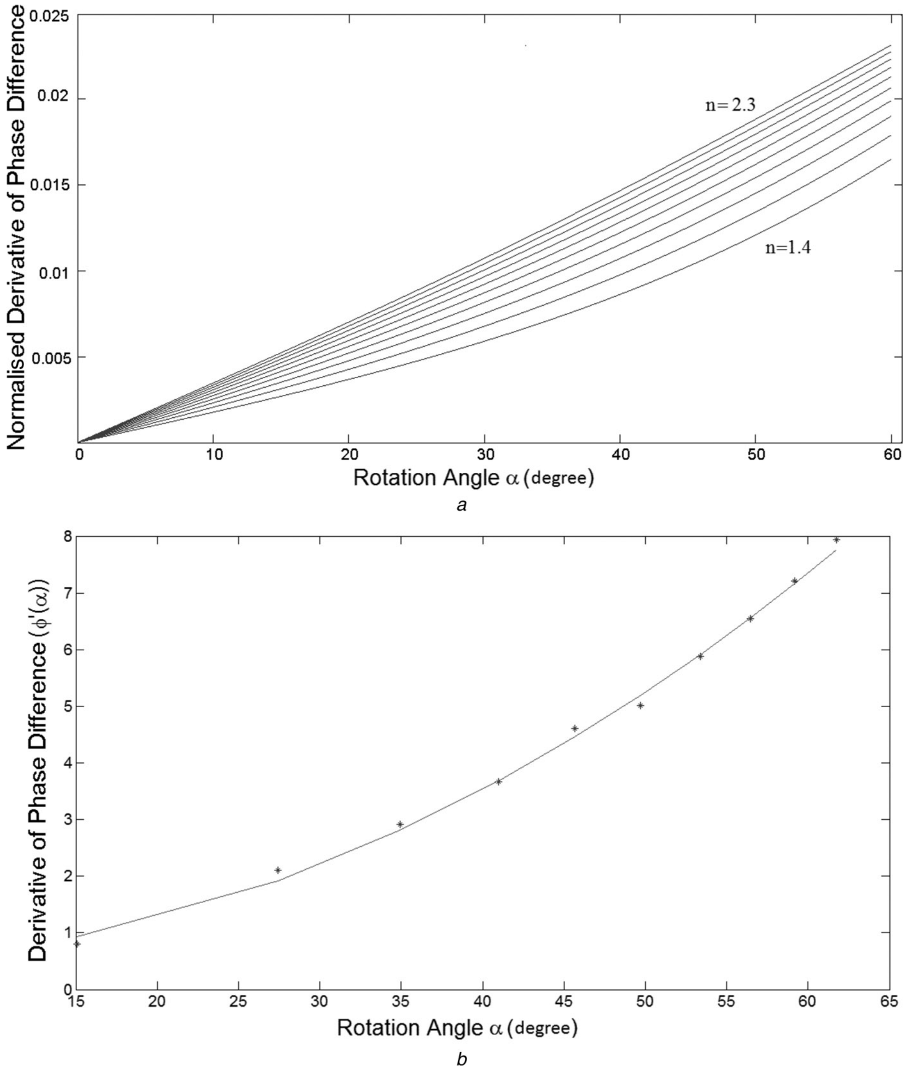

Fig. 3 *Normalised and experimental derivative of phase difference for a range of refractive index as a function of the rotation angle* α

a Normalised derivative of phase difference, $(kd)^{-1}\phi'(\alpha)$ for a wide range of refractive index from $n = 1.4$ to 2.3

b Experimental derivative of phase difference for $n = 1.34$ and $d = 55$ μm

Q2

value on the right-hand side of (4) to the experimental data, and thus compute kd.

The graph of normalised derivative $\phi_s'(\alpha)$, calculated from (4), is shown in Fig. 4 for different refractive indexes.

An interesting feature of $\phi_s'(\alpha)$ is that the trend is nearly parabolic (Fig. 4) and, more important, a minimum is found between 30 and 60°, which is nearly independent from n (at least in the range $n = 1.4$–2.3). Taking advantage of the symmetry, we can now pick two values of α located symmetrically with respect to the minimum, let us say α_1 and α_2, such that $\phi_s'(\alpha_1) = \phi_s'(\alpha_2)$. Then, using (4) for α_1 and α_2, and subtracting term by term, we obtain

$$\begin{aligned} 0 &= \phi_s'(\alpha_2) - \phi_s'(\alpha_1) \\ &= (\mathrm{kd})^{-1}[\phi'(\alpha_2) - \phi'(\alpha_1)] - 2\sin\alpha_2 + 2\sin\alpha_1 \end{aligned}$$

and we can solve for kd as

$$\mathrm{kd} = [\phi'(\alpha_2) - \phi'(\alpha_1)]/2[\sin\alpha_2 - \sin\alpha_1]$$

using the experimental values of the derivative $\phi'(\alpha)$, and of course angle α, we can then calculate the desired kd and finally multiply by $\lambda/2\pi$ to obtain d.

Even better, instead of using just a pair of α-values, we can extract all the relevant information carried by the experimental curve by filling the available interval of α-values around the minimum α_v by pairs of angles symmetrically located off $\pm m\Delta\alpha$ (where $m = 1\cdots p$ for say p pairs) and take the mean value of kd over the p pairs

$$\begin{aligned} d = \frac{1}{2k}\sum_{m=1}^{p} ((\phi'(\alpha_v + m\Delta\alpha) \\ - \phi'(\alpha_v - m\Delta\alpha))/(\sin(\alpha_v + m\Delta\alpha) - \sin(\alpha_v - m\Delta\alpha))) \end{aligned} \quad (5)$$

For a known refractive index, pairs of angles located symmetrically to the minimum are chosen from curves shown in Fig. 4, and then d is computed by (5). Once we find d, we can go back with it in (2) and calculate n. Then we can re-enter the loop of calculation until d and n are no more changed after iteration. Usually, as the α-minima (Fig. 4) are almost the same, two to three iterations are enough to converge to less than 2% of the final values.

doi: 10.1049/iet-opt.2011.0044

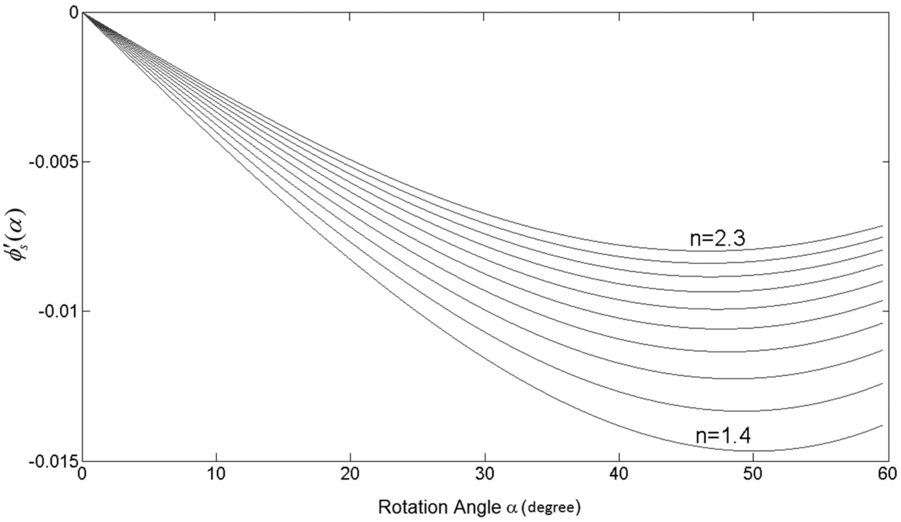

Fig. 4 *Graph of ϕ_s' (a) as a function of rotation angle α*

5 Iteration algorithm

For more details of the procedure, we further report the steps of the calculations of d and n using the derivative-based approach (5). We start by considering an initial interval ($[\alpha_1 - p\Delta\alpha,\ \alpha_1 + p\Delta\alpha]$) in the range of $30^\circ - 60^\circ$ to begin the first step of iteration algorithm, where α_1 is supposed to be a primary value of α_v, and p is the number of steps we use with discretisation $\Delta\alpha$. Then we subtract symmetric values of $\phi_s'(a)$ around $\alpha_v = \alpha_1$. As the result of the non-zero difference, we can introduce a deviation parameter Er of the d (5), defined as

$$\mathrm{Er} = \sum_{m=1}^{p} ((\phi_s'(\alpha_v + m\Delta\alpha) - \phi_s'(\alpha_v - m\Delta\alpha))/(\phi'(\alpha_v + m\Delta\alpha) - \phi'(\alpha_v - m\Delta\alpha))) \tag{6}$$

After calculating d_1 by (5) and substituting d_1 in (2) to obtain n_1, then (6) is used to optimise the α_v from an initial value to the next one. The iterative method then follows these steps:

1. Use n_j to find new angle of minima ($\alpha_v = \alpha_{j+1}$) to improve Er. A suitable choice for angle of minima is shown in Fig. 5, where α_{j+1} can be easily found by n_j and then symmetric curve is chosen around α_{j+1}.
2. Using new symmetric curves and $\alpha_v = \alpha_{j+1}$, new value of thickness d_{j+1} is obtained by (5), and then n_{j+1} is calculated from (2) by LSM.

The iterative procedure can continue with new n until we reach a minimum value of Er. Since equations are almost linear, the iterative method rapidly converges after few iterations and the entire calculation is fast. As shown in Fig. 5, Er keeps down to a low value on a wide range of refractive index, for example, $\mathrm{Er} < 0.05$ at $\alpha_v = 49.5^\circ$.

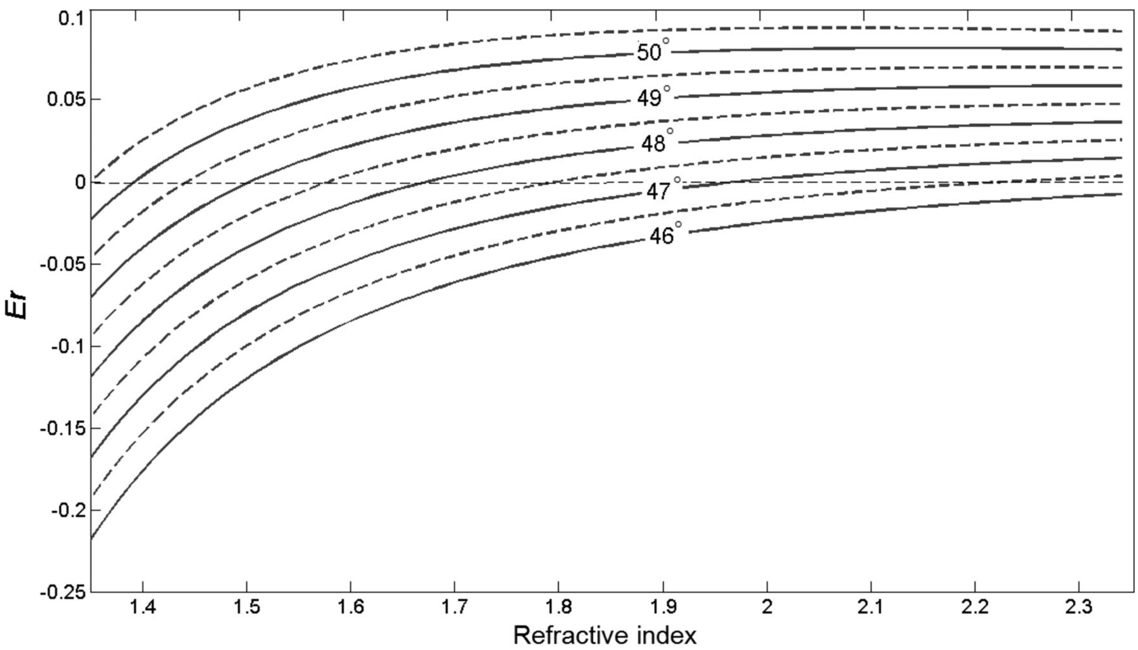

Fig. 5 *Deviation parameter (Er) respect to refractive index for different α_v*

Table 1 Samples measured by SMI

Nominal thickness and refractive index			Self-mixing measurement	
Thickness, D, μm, ±3%	Refractive index n, ±1%		Thickness $d \pm \Delta d$, μm	Refractive index $n \pm \Delta n$
1020	1.52	glass	1010.0 ± 10.0	1.515 ± 0.010
160	1.52	glass	162.5 ± 2.0	1.510 ± 0.015
75	1.58	PET	81.0 ± 0.5	1.570 ± 0.015
55	1.34	FEP	60.0 ± 0.5	1.330 ± 0.015
10	1.52	glass	10.6 ± 0.5	1.530 ± 0.020

To test the method, some samples of glass slab and polymer films [polyethylene terephthalate (PET) and fluorinated ethylene propylene (FEP)] provided by commercial suppliers were used. Surfaces were not treated to improve the finish, because the SMI tolerates some wave-front distortion [2].

It is worth noting that spatial resolution is determined by the small size (1 mm) of the beam.

Thickness values of samples presented in the left column of Table 1 were also carefully checked by a mechanical caliper. Accuracy of mechanical caliper was about 1 μm and was limited by sample rigidity.

As an example, for a glass sample with $n = 1.52$ and $d = 160$ μm, we started with an initial pair around $\alpha_1 = 47.5^\circ$ with $\Delta\alpha = 0.1^\circ$ and $m = 100$. The first thickness obtained by (5) was $d_1 = 154.4$ μm, and then $n_1 = 1.58$ using (2) and $\mathrm{Er}_1 = 0.036$ from (6). The first iteration was done with a new value of $\alpha_2 = 48.5^\circ$ where Er is minimised for $n_1 = 1.58$. Using this value for α_2, calculation of thickness gives $d_2 = 159.7$ μm, and then $n_2 = 1.53$ and $\mathrm{Er}_2 = -0.01$. At the second iteration $\alpha_2 = 49^\circ$, where Er is minimum for $n_2 = 1.53$. We got results converging to $n_3 = 1.51$, $d_3 = 162.5$ μm and $\mathrm{Er}_3 = 0.005$. Further iterations did not improve the result any further.

For all samples measured, one or two iterations were found enough to converge to the final result. Table 1 shows the self-mixing results for several thickness and refractive index, compared to results of a mechanical measurement with a caliper.

In order to evaluate the repeatability of measurement, we repeated it several times starting from the measured waveform (that in Fig. 1), and found a deviation of 0.01° in α and for Δd and Δn the values given in Table 1, that is, ±1% and 0.02 (rms), respectively.

As a final remark, going to [2] to make a comparison, we find that results obtained there are about in the same range of thickness, 10–1000 μm, but uncertainty of the measurement was a large ±2% or twice as much the repeatability obtained with the new SMI method proposed in this paper. Also, the uncertainty of an index of refraction
Q3 measurement was estimated in 0.1, respect to the 0.02 of this paper. A good reason for the difference is that we have introduced a relatively efficient processing of measured data in this paper, one able to exploit the full content of information contained in them, especially at a large incidence angle. In contrast, the double-channel SMI + LSI method of [2] starts from potentially more information content because of the double phase shifts collected in the experiment, but suffers from impairment because of the limited angle swing allowed from the LSI channel.

6 Conclusion

We have presented a new method to measure thickness and refractive index of transparent samples with a single-channel SMI. By analysing of derivative phase difference and using a simple iteration method, we have been able to determine both refractive index and thickness, and have achieved a relative repeatability estimated in 1% of thickness and 0.02 in refractive index. The method is very easy to implement in the laboratory and requires only a few simple components.

7 Acknowledgment

One of us (M.T. Fathi) wish to thank the Abdus Salam International Center for Theoretical Physics (ICTP), Trieste, Italy, for partial support of his scholarship.

8 References

1 Coppola, G., Ferraro, P., Lodice, M., Nicola, S.D.: ‘Method for measuring the refractive index and the thickness of transparent plates with lateral-shear, wavelength-scanning interferometer’, *Appl. Opt.*, 2003, **42**, (19), pp. 3882–3887

2 Fathi, M.T., Donati, S.: ‘Thickness measurement of transparent plates by a self-mixing interferometer’, *Opt. Lett.*, 2010, **35**, (11), pp. 1844–1846

3 Giuliani, G., Norgia, M., Donati, S., Bosch, T.: ‘Laser diode self-mixing technique for sensing applications’, *J. Opt. A, Pure Appl. Opt.*, 2002, **4**, pp. 283–294

4 Donati, S., Giuliani, G., Merlo, S.: ‘Laser diode feedback interferometer for measurement of displacements without ambiguity’, *IEEE J. Quantum Electr.*, 1995, **31**, (1), pp. 113–119

5 Xi, J., Yu, Y., Chicharo, J., Bosch, T.: ‘Estimating the parameters of semiconductor lasers based on weak optical feedback interferometry’, *IEEE J. Quantum Electr.*, 2005, **41**, (8), pp. 1058–1064

6 Donati, S.: ‘Developing self-mixing interferometry for instrumentation and measurements’, *Laser Photonics Rev.*, 2011, **5**, doi: 10.1002/lpor.201100002, in press Q4

7 Donati, S.: ‘Electro-optical instrumentation – sensing and measuring with lasers’ (Prentice Hall, USA, 2004)

doi: 10.1049/iet-opt.2011.0044